Fracture of Hard Thin Films Using Nanoindentation and Nanoscratch Techniques: A Materials and Mechanics Approach

N. R. Moody, D. Medlin, R. Q. Hwang, D. Boehme,
S. Venkataraman , and W. W. Gerberich
Sandia National Laboratories, Livermore, CA 94550
** Applied Materials, Santa Clara, CA 94520
** University of Minnesota, Minneapolis, MN 55455

SAND--98-8504C
CONF-980627--

Thin films are used in many applications where special properties are needed to insure performance and reliability. Of particular interest are thin tantalum nitride films. They are used extensively in microelectronic applications because of their long term stability and low thermal coefficient of resistance. [1,2] They are sputter deposited which produces films with a high structural defect content and high compressive residual stresses both of which can alter the physical and mechanical properties of microelectronic thin films. [3,4] Although these films are strong heat generators, they exhibit no changes in structure or composition of the interface with aluminum oxide substrates that degrade performance or reliability. [5] However, the use of high power density components is driving a move to replace aluminum oxide with aluminum nitride for greater heat transfer. [6] This replacement substrate creates concern as residual stresses and long-term operation could induce detrimental changes along the thin film interface not observed in aluminum oxide devices. As a result, we employed nanoindentation [7,8] and continuous nanoscratch testing [9,10] to determine the effects of the intrinsic compressive residual stresses on the properties and fracture resistance of the thin tantalum nitride films. These techniques sample small volumes of material while preserving the production configuration of a free surface. Although nanoscratch tests lack a rigorous derivation of stress distributions and strain energy release rates [9,10], good approximations for strain energy release rates can be obtained using mechanics-based models for blister formation where residual stresses dominate interfacial fracture behavior. [11,12] When combined with scanning and transmission electron microscopy, the results define structure-property relationships and resistance to fracture of these hard films.

The thin tantalum nitride films used in this study were reactively sputtered onto smooth sapphire (single crystal alumina) substrates and air-fired aluminum nitride substrates. The sapphire substrates were prepared by heating to 170°C in vacuum for two hours to drive off moisture followed by an RF backsputter for 120 s to remove contaminants and expose fresh material. The aluminum nitride substrates were air fired at 850°C for one hour to produce a surface oxide. They were then heated to 170°C in vacuum for two hours to drive off moisture followed by an RF backsputter for 15 s to clean the surface. With a vacuum maintained to less than 1.3×10^{-5} Pa (10^{-7} torr), films were deposited at a rate of 0.3 nm/s on both types of substrates using a tantalum target, argon as a carrier gas, and controlled additions of nitrogen to form Ta_2N. The final film thicknesses were 635 nm on the sapphire substrate, and 160, 440 and 500 nm on the aluminum nitride substrates. [13,14]

Nanoindentation tests showed that the elastic moduli of all films were equal to 350 GPa which closely matches the elastic moduli of both the sapphire and aluminum nitride substrates. The hardness values for the films were near 35 GPa which are somewhat higher than the 26 GPa measured for sapphire and much higher than the 16 GPa measured for aluminum nitride. [13,14]

Cross-sectional TEM of the 635 nm thick films on sapphire substrates revealed that the first 200 nm of the film is amorphous. At distances greater than 200 nm from the aluminum oxide-tantalum nitride interface the film develops a pronounced preferred orientation with the basal plane of the film perpendicular to the substrate and the microstructure exhibiting a tapered columnar structure. (Figure 1a) The films on aluminum nitride have the same relatively smooth surface and structure as the films on the sapphire substrate. High Resolution TEM showed that the interfaces in all films have a three to four atom layer transition region extending from the aluminum oxide substrate into the tantalum nitride film. Although it appears amorphous there is a periodicity to the interface structure indicating either a transition or periodic array of defects. (Figure 1b) [13,14]

The sputter deposition did produce a high structural defect content and high compressive residual stresses which can change with time and adversely affect reliability. Following the approach of Sun, Tisone, and Cruzan [3], the change in lattice parameters for (0002), ($10\bar{2}1$), and ($10\bar{3}2$) x-ray diffraction peaks from corresponding unstressed tantalum nitride values were used to estimate in-plane residual stresses as follows,

$$\sigma = \frac{E}{2\nu}\frac{a_o - a}{a_o} \qquad (1)$$

where a_o and a are the measured lattice parameters of the unstressed standard and stressed film respectively, v is Poisson's ratio taken as 0.35, and E is the measured elastic modulus. All films exhibited a lattice parameter increase normal to the film surfaces revealing in-plane compressive stresses that increased with film thickness. The data are given in Table I.

A series of ten nanoscratch tests were run on each film to determine resistance to fracture. In all tests, the point of fracture was characterized by an abrupt increase in tangential load. This is shown for the as-deposited film on a sapphire substrate in Figure 2a. Beyond the initial point of fracture, the indenter penetrated the aluminum nitride substrate. The fractures were always characterized by well-defined spalls along the film and substrate interface. (Figure 2b) Fracture of the films on aluminum nitride substrate occurred at lower loads and was accompanied by smaller spalls than in films on sapphire as shown in Figure 3. Compositional scans across the fracture surfaces showed no evidence of tantalum from the film suggesting that

DISCLAIMER

fracture occurred along either the interface or just within the sapphire or aluminum nitride substrates.

The energy stored in each film at fracture was estimated as follows,

$$G^* = \frac{(1-\nu)\sigma_r^2 h}{E} + \Sigma\left(\frac{(1-\nu)\bar{\tau}_{ij}^2 h}{\mu} + \frac{(1-\nu)\bar{\sigma}_{ij}^2 h}{E}\right) \quad (2)$$

where G^* is the stored elastic strain energy available for fracture, h is the film thickness, E is the elastic modulus and μ is the shear modulus of the film, σ_r is the residual stress in the film, and $\bar{\tau}_{ij}$ and $\bar{\sigma}_{ij}$ are the average applied elastic shear and normal stresses in the film at fracture. [10,13] The energies expended for fracture and phase angles of loading were determined using the circular blister analysis of Hutchinson and Suo. [12,13] The stored energies and energies expended on fracture are comprised of mode I and mode II contributions. Treating interfacial fracture as a mode I failure [15], the mode I contributions to fracture were estimated using the following relationship [12],

$$\Gamma_I = \Gamma_{I\text{-}II}/(1+\tan^2\psi) \quad (3)$$

where $\Gamma_{I\text{-}II}$ is the measured fracture energy, ψ is the phase angle of loading, and Γ_I is the projected mode I fracture energy.

The results for the tantalum nitride films on aluminum nitride substrates in this study are given in Table I. This table shows the loads at fracture and fracture areas differed with substrate and with film thickness as did the applied energies. Furthermore, it is shown that a reduction in residual stress combined with a decrease in film thickness markedly reduced the residual stored energy in the thinnest film tested. In all cases, the mode I fracture energies ranged from 1.3 to 3.9 J/m^2 which are typically associated with chemical or metallic bonding. However, the values for fracture on sapphire substrates were nearly a factor of two higher than for fracture on aluminum nitride substrates even though the aluminum nitride surface forming the interface with the films was covered by a layer of aluminum oxide. This suggests that strain energy release rates may differ between substrates due to differences in plastic energy dissipation and should not be ignored. This highlights the need for continued advances in testing techniques and efforts in model development to provide physically accurate and quantitatively correct descriptions of the fracture process in thin tantalum nitride films.

Acknowledgments:

This work supported by U.S. DOE Contract DE-AC04-94AL85000. S. Venkataraman and W. W. Gerberich gratefully acknowledge the support of the Center for Interfacial Engineering at the University of Minnesota under grant NSF/CDR-8721551. W. W. Gerberich also acknowledges support of the U. S. DOE through Contract DE-FG02-96ER45574.

References:

[1] Adams, J. R. and Kramer, D. L., "A Study of the Oxidation of Tantalum Nitride by Ellipsometry and Auger Electron Spectroscopy", Surface Science 56, 482-487, 1976.

[2] Au, C. L., Anderson, W. A., Schmitz, D. A., Flassayer, J. C., and Collins, F. M., "Stability of Tantalum Nitride Thin Film Resistors", J. Mater. Res., 5 , 1224-1232, 1990.

[3] Sun, R. C., Tisone, T. C., and Cruzan, P. D., "The Origin of Internal Stress in Low-Voltage Sputtered Tungsten Films", J. Appl. Phys., 46, 112-117, 1975.

[4] E. Klokholm, " Effects of Stress on the Physical Properties of Thin Films", J. Vac. Sci. Technol. 8 , 148-151, 1971.

[5] Zhao, X.-A., Kolawa, E., and Nicolet, M.-A., "Reaction of Thin Metal Films With Crystalline and Amorphous Al_2O_3", J. Vac. Sci. Technol. A , 4, 3139-3141, 1986.

[6] Garrou, P., "Aluminum Nitride for Microelectronic Packaging", Advancing Microelectronics, 21, 6-10, 1994.

[7] Doerner, M. F. and Nix, W. D., "A Method for Interpreting the Data from Depth-Sensing Indentation Instruments", J. Mater. Res., 1, 601-609, 1986.

[8] Oliver, W. C. and Pharr, G. M., "An Improved Technique for Determining Hardness and Elastic Modulus Using Load and Displacement Sensing Indentation Experiments", J. Mater. Res., 7, 1564-1583, 1992.

[9] Wu, T. W., "Microscratch and Load Relaxation Tests for Ultra-Thin Films", J. Mater. Res., 6, 407-426, 1991.

[10] Venkataraman, S. K., Kohlstedt, D. L., and Gerberich, W. W., "Metal-Ceramic Interfacial Fracture Resistance Using the Continuous Microscratch Techniques", Thin Solid Films, 223, 269-275, 1993.

[11] Marshall, D. B., and Evans, A. G., "Measurement of Adherence of Residually Stressed Thin Films by Indentation Mechanics of Interface Delamination", J. Appl. Phys., 56, 2632-2638, 1984.

[12] Hutchinson, J. W., and Suo, Z., "Mixed Mode Cracking in Layered Materials", In Advances in Applied Mechanics, 29, Ed. Hutchinson, J. W. and Wu, T. Y., Academic Press, Inc., New York, pp. 64-191, 1992.

[13] Moody, N. R., Hwang, R. Q., Venkataraman, S. K., Angelo, J. E., Norwood, D. P., and Gerberich, W. W., "Adhesion and Fracture of Tantalum Nitride Films", Acta Materialia, 46, 585-597, 1998.

[14] Moody, N. R., Medlin, D., Boehme, D., and Norwood, D. P., "Film Thickness Effects on the Fracture of Tantalum Nitride on Aluminum Nitride Thin Film Systems, submitted to Engineering Fracture Mechanics, 1998.

[15] Evans, A. G., Ruhle, M., Dalgleish, B. J., and Charalambides, P. G., "The Fracture Energy of Bimaterial Interfaces", In Metal-Ceramic Interfaces, Ed. Ruhle, M., Evans, A. G., Ashby, M. F., and Hirth, J. P., Pergammon Press, Oxford, pp. 345-364, 1990.

Table I. The applied, residual stress, and total stored strain energies at fracture, $G_{applied}$, $G_{residual}$, and G_{total}, and the energies expended on fracture, Γ_{I-II}, the phase angles of loading, ψ, and projected mode I fracture energies, Γ_I, along with areas of spallation, A, and the critical normal and tangential loads for fracture, P_{cr} and L_{cr}, from scratch tests on as-deposited thin tantalum nitride films.

Film/Thickness	A (mm^2)	P_{cr} (mN)	L_{cr} (mN)	σ_{res} (GPa)	G_{res} (J/m^2)	G_{appl} (J/m^2)	G_{total} (J/m^2)	Γ_{I-II} (J/m^2)	ψ	Γ_I (J/m^2)
Ta_2N/Al_2O_3										
635 nm	210	98	60	-5.4	34.7	0.4	35.1	15.5	-60	3.9
Ta_2N/AlN										
500 nm	107	102	53	-4.5	18.8	0.6	19.4	4.3	-51	1.6
440 nm	82	87	47	-4.7	17.1	0.3	17.4	6.4	-56	1.8
160 nm	9	26	17	-3.8	4.3	17.9	22.2	9.8	-61	1.3

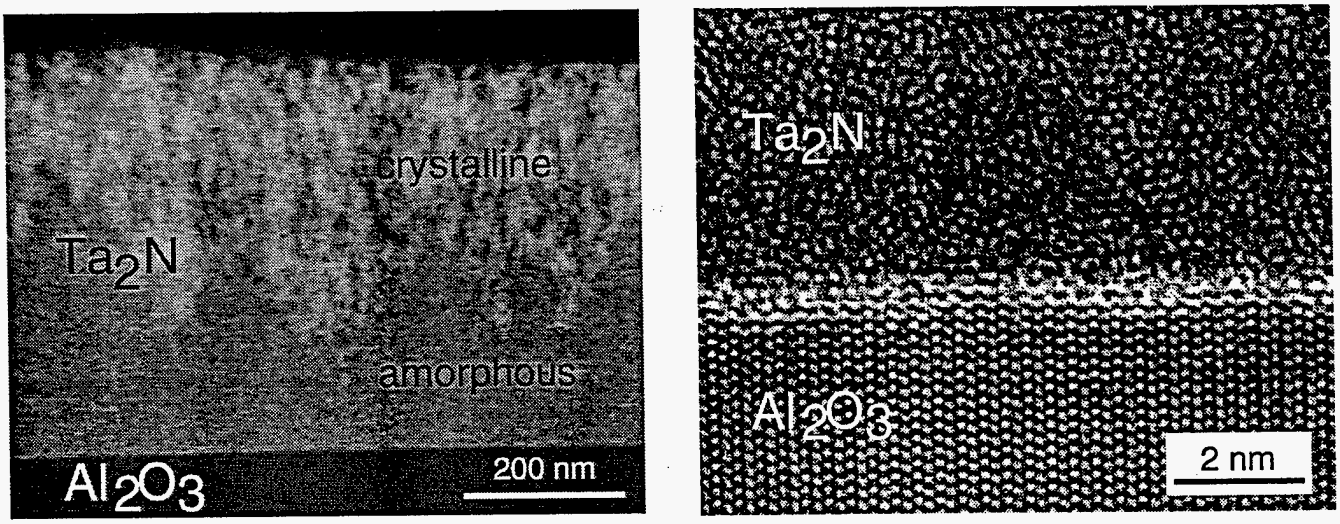

(a) (b)

Fig. 1. The microstructure of as-deposited films (a) consists of a 200-nm-thick amorphous region near the interface followed by columnar grains extending to the film surface. The interface between the film and substrate (b) is characterized by a three-to-four atom-layer transition from an amorphous to crystalline structure.

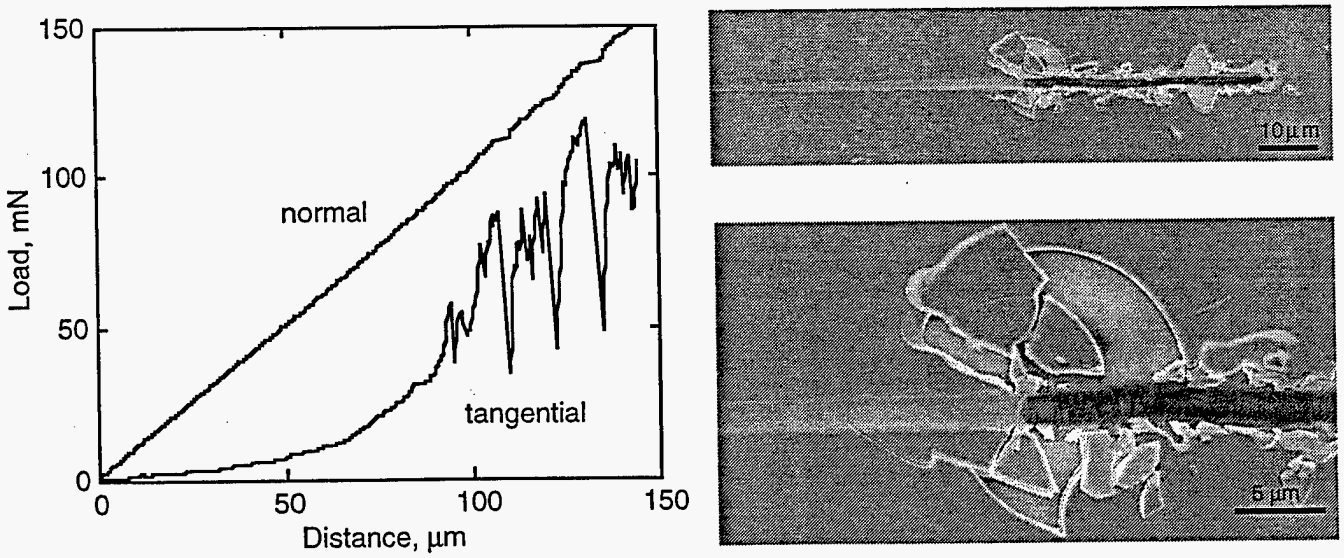

(a) (b)

Fig. 2. Scratch test fractures in the as-deposited film on sapphire (a) occurred consistently near 100 mN and were characterized by an abrupt increase in tangential load. (b) The fractures propagated along the film-substrate interfaces producing well-defined spalls ahead of the indenter.

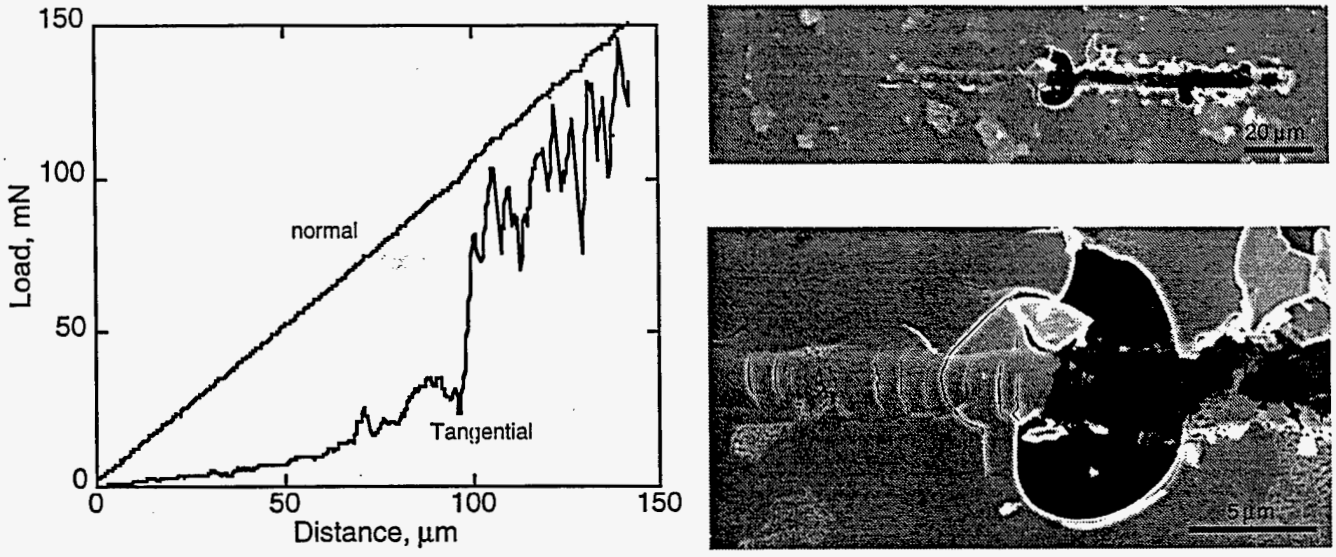

Fig. 3. Scratch test fractures in the as-deposited films on aluminum nitride (a) were also characterized by abrupt increases in tangential load and indenter depths producing (b) well-defined spalls ahead of the indenter. This figure is from fracture in the 440-nm-thick as-deposited film.

Report Number (14) SAND--98-8504C
CONF-980627--

Publ. Date (11) 19980319
Sponsor Code (18) DOE/DP , XF
JC Category (19) UC-704 , DOE/ER

DOE